



HAL
open science

High efficiency parallel-parallel LLC resonant converter for HV/LV power conversion in electric/hybrid vehicles

Gang Yang, Pierre Sardat, Patrick Dubus, Daniel Sadarnac

► To cite this version:

Gang Yang, Pierre Sardat, Patrick Dubus, Daniel Sadarnac. High efficiency parallel-parallel LLC resonant converter for HV/LV power conversion in electric/hybrid vehicles. PCIM Europe 2014, May 2014, Nuremberg, Germany. pp.1-9. hal-01102413

HAL Id: hal-01102413

<https://centralesupelec.hal.science/hal-01102413>

Submitted on 12 Jan 2015

HAL is a multi-disciplinary open access archive for the deposit and dissemination of scientific research documents, whether they are published or not. The documents may come from teaching and research institutions in France or abroad, or from public or private research centers.

L'archive ouverte pluridisciplinaire **HAL**, est destinée au dépôt et à la diffusion de documents scientifiques de niveau recherche, publiés ou non, émanant des établissements d'enseignement et de recherche français ou étrangers, des laboratoires publics ou privés.

High efficiency parallel-parallel LLC resonant converter for HV/LV power conversion in electric/hybrid vehicles

Gang YANG, VALEO, France, yjsyanggang@gmail.com
 Pierre SARDAT, VALEO, France, pierre.sardat@valeo.com
 Patrick Dubus, VALEO, France, patrick.dubus.ext@valeo.com
 Daniel Sadarnac, Ecole Supérieure d'Electricité, France, daniel.sadarnac@supelec.fr

Abstract

The design of a hybrid/electric automobile oriented 2.5kW, 250kHz, HV/LV double phase parallel-parallel connected LLC resonant converter is presented. This paper proposed the concept of double phase LLC with its double loop control strategy to share the power equally between the two power cells and to maintain a high efficiency among a wide output power range. Design considerations, including the MOSFETs power module, magnetic components integration and air-cooling system are presented in detail. The final developed prototype, which can almost be directly industrialized, is targeted for future utilization in electric vehicles/hybrid vehicles. The total prototype performs 3kg, 2.5L, and a high power density 1W/cm³. Experimental results prove that a peak efficiency of 95% is obtained and efficiency is above 94% from 500W to 2kW.

1. Introduction

In electric or hybrid vehicles, a step-down DC/DC converter is used to produce a low voltage net to power all vehicle standard equipments, shown as in the Fig.1.

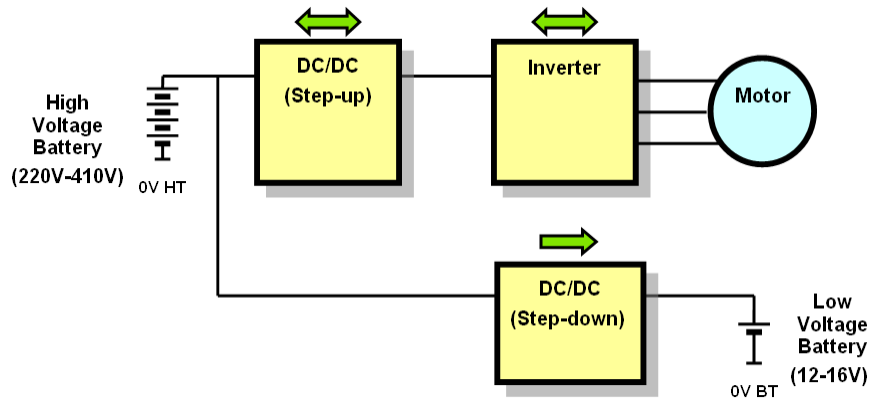


Fig.1: Electric power flow in an electric/hybrid vehicle

For safety reasons, high voltage equipments are floating from vehicle chassis ground and electrical insulation between high voltage and low voltage batteries should be assured. The high voltage battery fluctuates between 220V to 410V and the low voltage battery fluctuates from 12V to 16V, depending on its state of charge. The converter may operate at any power from 0 to 2.5kW, however, the following two power ranges: 600-900W and 1.5-1.8kW are more frequently utilized. Improving conversion efficiency at the two specified power ranges has particular interests in improving the converter's overall performance.

During all the available topologies, LLC topology is a good candidate which performs soft-switching at wide load range, improved EMC performances and reduced magnetic component size [1]. In LLC, zero voltage switching-discontinuous current mode (ZVS-DCM)

is highly preferred than ZCS mode or ZVS-CCM mode due to limited frequency range and higher power factor [2]. The main drawback of LLC is its inability to compromise high efficiency with large input/output voltage variation. Efficiency is greatly sacrificed by enlarging its input/output voltage range. In this case, a pre-regulation stage (Boost for example) could be used as the first stage to broaden the input voltage range. The input voltage variation range of the targeted LLC prototype thus is reduced to 330V-410V to get higher efficiency and high power factor. To measure and validate the converter's efficiency, the prototype is regulated to a constant output voltage.

2. Topology and Control

For HV/LV power conversion, LLC resonant converter generally keeps a very competitive efficiency in designing DC/DC power supplies in low or medium power level [3-5]. The reported LLC resonant converters in literatures are generally between 300W and 1kW. Increasing load brings the following difficulties: the first difficulty lies in the transformer core realization. With the increase of power, the transformer's magnetizing inductance decreases linearly. Low magnetizing inductance makes the transformer core difficult to be realized practically by a reasonable air-gap length. Secondly, single cell LLC converter performs a very poor power factor at light load, which causes more conduction loss and deteriorates the power conversion efficiency. In view of all the above limitations of single cell LLC, the parallel-parallel connected topology with each power cell at half of the total power, is proposed in this prototype to solve the above two shortcomings, with regard to Fig.2.

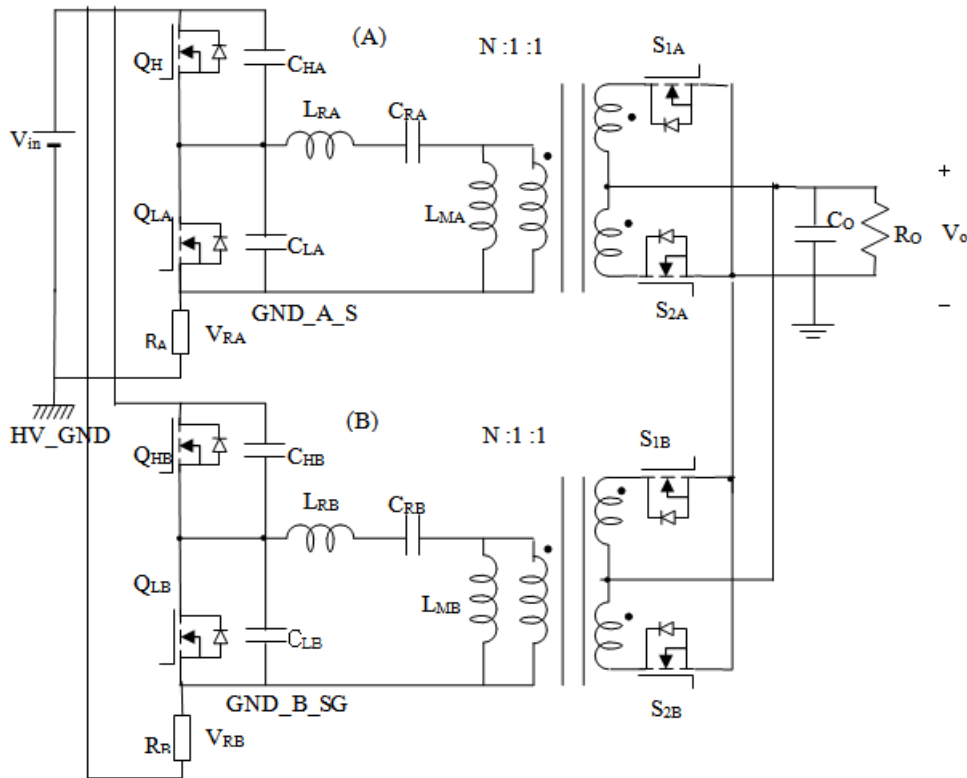


Fig.2. Proposed double phase parallel-parallel LLC topology to handle high power

The double phase LLC resonant converter contains two resonant cells in parallel, noted as cell (A) and cell (B), separately. Traditional control method is to operate both the two phases at the same frequency with one same controller driver; a phase shift of 90° between adjacent cells is implemented to get an output current with fewer ripples [6]. However, resonant cell component mismatch causes the two cells to exhibit different voltage conversion ratios at the

same frequency; as a result, the load current is no longer equally distributed. In order to assure an equal current sharing between two cells, a novel control method is proposed in this paper, shown as in Fig.3:

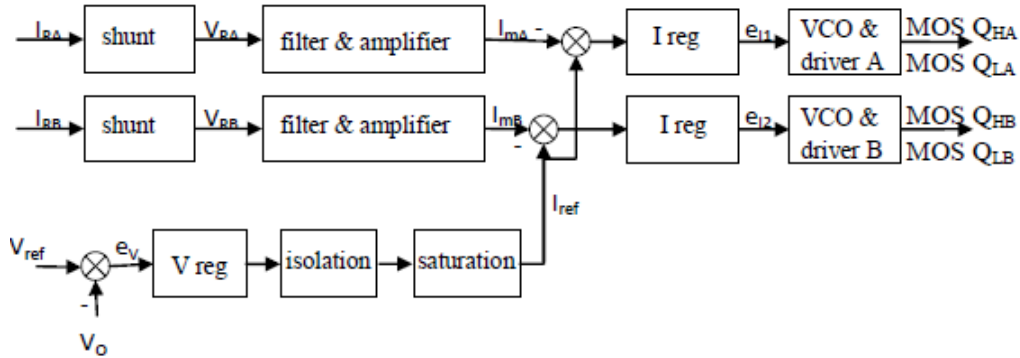


Fig.3. Bloc diagram of the control strategy for input current balancing

Proposed control circuit strategy is to adopt a double loop control method: an external output voltage control for output voltage regulation and an internal current control for input current balancing. The input current of each power cell is sensed by resistive shunts R_A and R_B , separately. The sensed signals are filtered and amplified to a suitable level (noted as I_{mA} and I_{mB}) and they reflect the average input current of each cell. As the reference current I_{ref} for both the two power cells are equal, this control method assures an equal input current distribution among the two power cells. Component value dispersion enables the two power cells to operate at two frequencies slightly different to perform the same voltage conversion ratio and thus the input current between two cells can be equally shared.

The proposed double cell topology and control strategy brings also the following advantages: firstly, at light load ($P < 1.1\text{kW}$), high conversion efficiency can be assured by switching off one power cell. A special cell switching logic is applied to further ensure an equal aging speed of the two power cells by switching off cell A or B following a given sequence. Secondly, at high load, when one power cell is off by incident, the other cell's power is limited by the saturation of reference signal I_{ref} ; this avoids all the power passes through another cell and the power components are protected from over-current problems. Thirdly, as switching frequencies for two cells are slightly different and the EMC noise levels are the same, one can design the input/output filters based on the noise emitted by one cell, the other cell benefits the same attenuation at an adjacent frequency.

Loop stability is analyzed by circuit modeling in Simplis software, based on which the regulator parameters can be designed to get a system precise, rapid and stable.

As for the circuit dimensioning, two 1.25kW LLC power cells are needed to be designed. The operation frequency range is 150kHz-250kHz, which is selected according to the various EMC specifications by automobile fabricants (The main EMC noise in LLC is doubled to 300kHz-500kHz, the frequency range where the highest noise level is authorized). The gain of a LLC converter including secondary leakage inductance L_2 is calculated and expressed by (1).

$$G = \frac{1}{\left(1 + \lambda - \lambda \frac{1}{f_n^2}\right) + jQ \left(\left(\frac{L_2}{L_m} \left(1 + \frac{1}{\lambda}\right) + 1 \right) f_n - \left(\frac{L_2}{L_m} + 1 \right) \frac{1}{f_n} \right)} \quad (1)$$

Where Q is the quality factor of the resonant converter; f_n is the switching frequency after normalization; f_r is the main resonant frequency; λ is the ratio between the leakage inductance and magnetizing inductance, L_2 is the secondary leakage inductance transferred to the primary side. At high power, low output voltage condition, the load resistance is rather low. The influence of transformer's secondary leakage inductance cannot be neglected as its

impedance is approaching the load resistance at high switching frequencies. The resonant tank's parameters shall be carefully selected according to equation (1) to compromise the gain requirement at the maximum and minimum operational frequency. Finally, the resonant cell parameters adopted in this prototype are: $L_r=7.5\mu\text{H}$, $L_m=42\mu\text{H}$, $C_r=50\text{nF}$.

3. Prototype Design Considerations

3.1. Magnetic Components Integration

In the converter prototype, the targeted magnetizing inductance is $L_m=42\mu\text{H}$. To create the required magnetizing inductance is not a problem, with 16 turns at the transformer's primary side, magnetic cores with a low inductance factor $A_L\approx 165\text{nH}$ should be selected. High leakage inductance is realized by separating the secondary windings from the primary windings. The adopted winding solution is by winding the 16 turns of primary winding (800x44AWG) at the center and secondary winding (1200x44AWG, 4 in parallel) at two extremities, shown as in Fig.4.

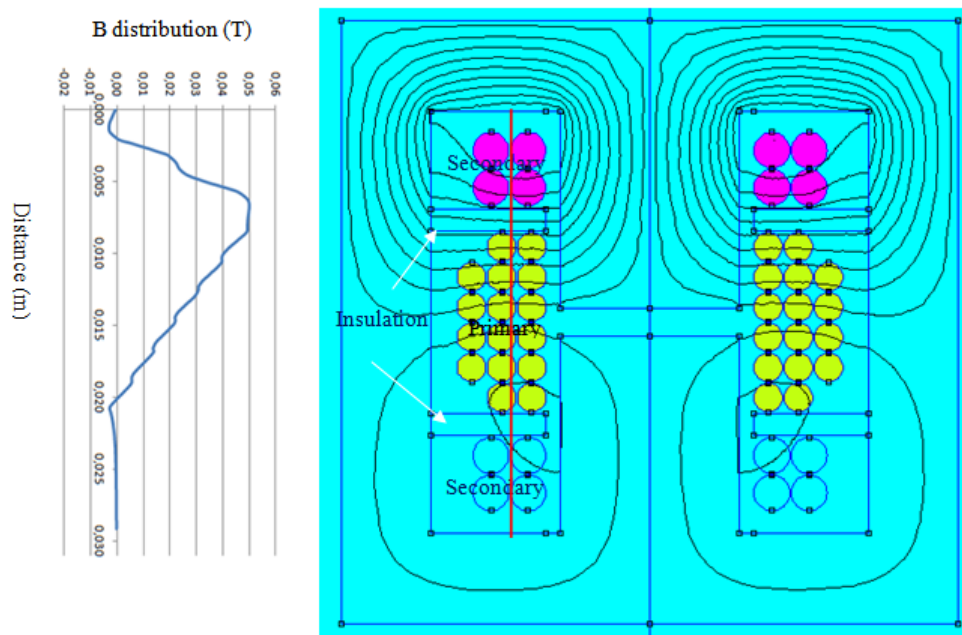


Fig.4. Leakage energy distribution for proposed transformer, $l_f=1.5\mu\text{H}$

The adopted core set is E42/21/15-3C97-A160. As shown in Fig.4, high flux density is detected at the insulation layer, $B_{pk}\approx 50\text{mT}$. With a large inter-space between primary and secondary side, this transformer performs a high leakage inductance of $l_f= 1.5\mu\text{H}$. The remaining resonant inductance of $6\mu\text{H}$ shall be completed by an additional RM12 core, with 6 turns. A photo of magnetic components is shown in the Fig.5.

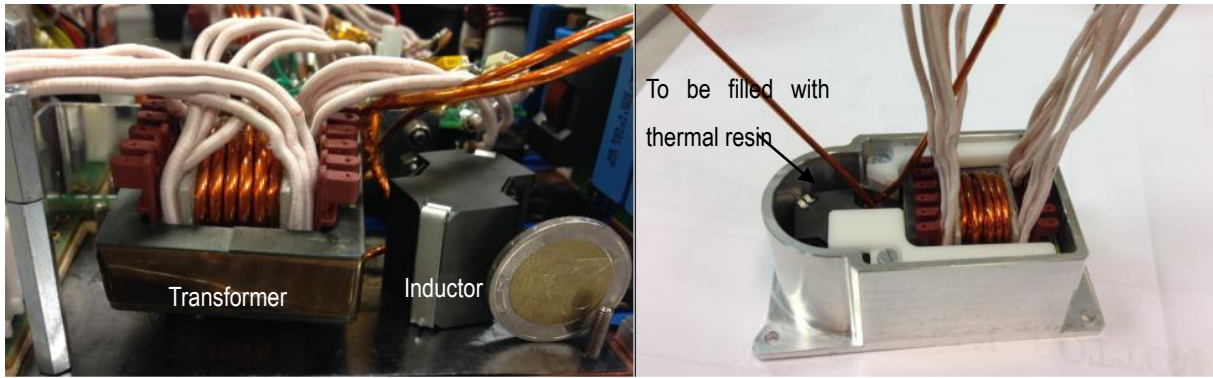


Fig.5. Transformer structure with additional resonant inductor RM12 without cooling container (left) and in a cooling container (right)

Litz wire is here used to avoid skin effect and reduce windings' proximity effect in transformer construction. In Litz wire, the diameter of each strand should be smaller than the skin depth. Under this condition the current distribution is expected to be homogenous at the section of each strand. However, considerably high loss can still be generated due to proximity effect. When Litz wire is exposed to an external magnetic field generated by transformer's air gap, fringing flux penetrates into the Litz wire and eddy current is generated at primary windings. Finer stands should be selected to minimize this eddy current loss. In this project, Litz wire 44AWG with diameter 50 μ m (around 1/3 of skin depth) is selected [7] and the simulation results are shown as follows:

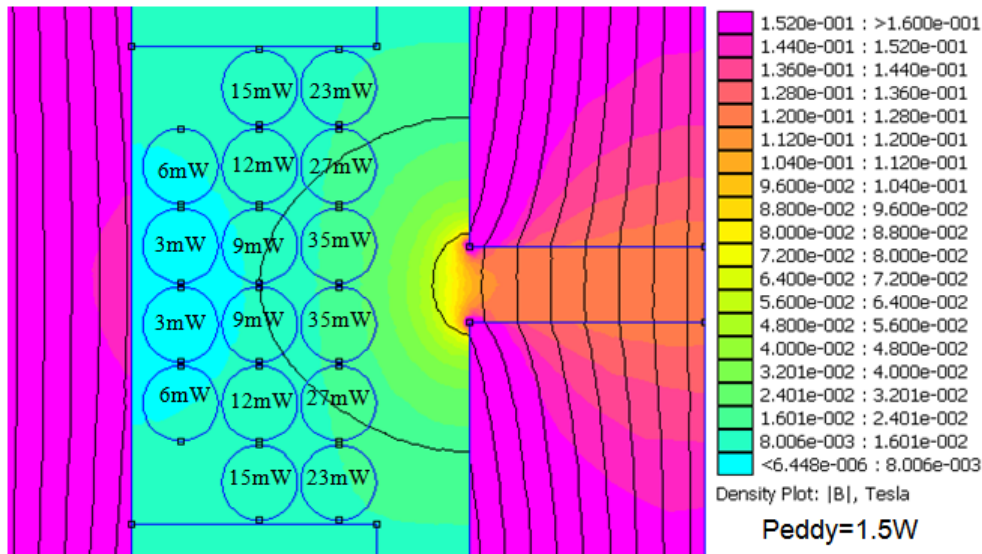


Fig.6. Eddy current loss simulation results at FEMM

The adopted solution to reduce the eddy-current loss is to increase the thickness of coil-formers and keep the windings away from air-gap. All the primary turns see a reduced magnetic field induction and the proximity effect can be reduced. The obtained eddy current loss under this case is 1.5W.

3.2. LV MOSFETs Integration

One challenge of this project is how to handle significant power loss caused by high output current circulating at LV MOSFETs. Standard discrete MOSFETs components are difficult to use here due to limited thermal conductivity and packaging interconnection resistance. More discrete MOSFETs should be paralleled in order to overcome this problem and this increases

the overall number of semiconductor devices and increases the overall volume. In this case, an interesting solution is to use a dedicated power module integrating all the LV MOSFETs. [8]

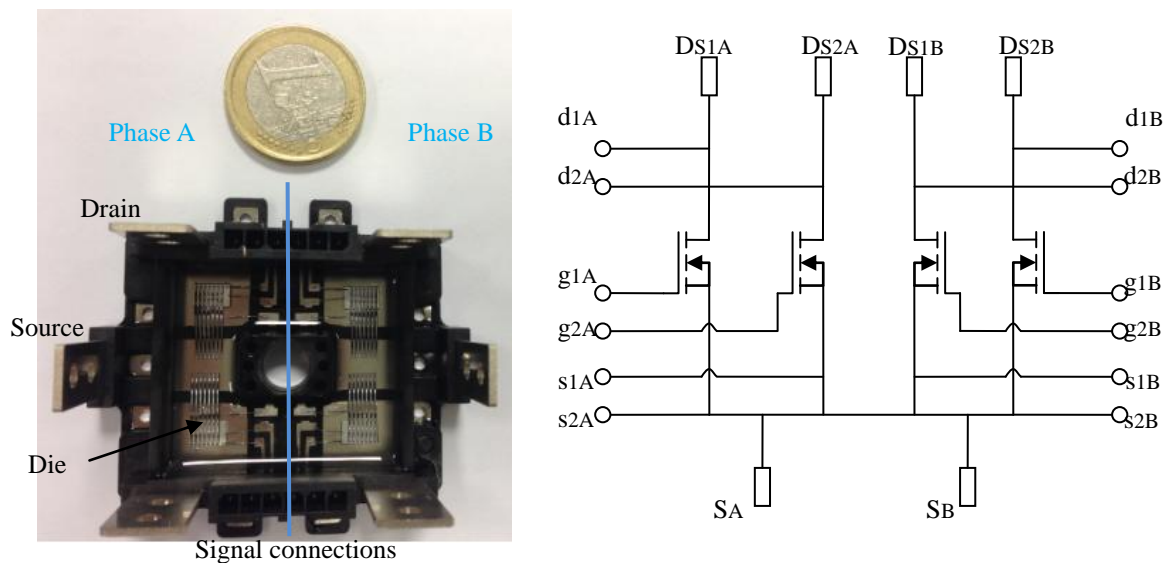


Fig.7. Populated LV IML power modules and its equivalent electrical circuit

In this project, an inserted molded lead-frame (IML) power module is designed, shown as in the above figure. Metal lead-frames are inserted into a plastic molding, which present horizontal open areas, where the MOSFETs dies are brazed on. The lead-frame also spreads to the outside, forming out electrical power connection terminals: four drain connections and two source connections. The designed power module consists of four dies arranged in a double phase configuration, as shown in the equivalent circuit. The die's source is connected to the lead-frame by a set of double stitch bondings ($7 \times 375 \mu\text{m}$). Small signal connections for synchronous rectification are drawn out by bondings $125 \mu\text{m}$. The power module itself is fixed to the cooling plate by screws and turnbuckles. The lead-frame is made up from copper of 0.8mm thickness for high electrical and thermal conductivity. The adopted bare die is Infineon IIPC22S4N06, with an internal resistance $R_{\text{dson}} = 1.3 \text{ m}\Omega$ and a breakdown voltage of $V_{\text{DSS}} = 60 \text{ V}$. The total resistance including metal lead-frame is less than $2 \text{ m}\Omega$.

A thermal interface (BFG30A, $c = 5 \text{ W/mK}$, $300 \mu\text{m}$) should be inserted below the power module to ensure an electrical insulation between lead-frame and cooling-plate. Through 3D simulation, the total thermal resistance from bare die to the cooling plate is: $R_{\text{thMI}} = 1.393 \text{ }^\circ\text{C/W}$. The designed IML power modules have significant advantages in thermal performances over discrete FET components.

3.3. Cooling system and prototype assemblage

As for air cooling, standard aluminum extrusions no longer have the capacity to sufficiently spread the power losses generated by electronic components and thus hot points exist. To design an efficient cooling system, the solution adopted here is by inserting a vapor chamber into the base of the heat sink [9], shown as in the Fig.8. The principles of evaporation and condensation in vapor chamber heat pipes produce a very high conductivity thermal plane. Like traditional cylindrical heat pipes, heat is evacuated using the working fluid, assuring a uniform temperature distribution and an elimination of hot spots. This is a great advantage of vapor chamber compared to traditional aluminum plate. Experimental results found that the temperature difference at vapor chamber's different positions is 4°C maximum versus 16°C maximum in copper plate at 22°C room temperature.

The following picture shows the components integration within the prototype. As the input

filter PCB's power loss is rather limited, it is mounted vertically to reduce the overall prototype area. HV MOSFETs are mounted directly to the vapor chamber and fixed by screws to improve the cooling effect. Thermal interfaces should be inserted between HV MOSFETs and the vapor chamber to realize electrical insulation. Magnetic components are arranged symmetrically in two phases and LV MOSFETs module is mounted on the vapor chamber directly. The control PCB board is mounted on the four spacers, above the power components. An external connection with 16 lines is used for exchanging control signals and export measurement results. After assembly, the prototype performs an overall volume of 2.5L (excluding the heat sink), 3kg and 2.5kW nominal power. The power density is $1\text{W}/\text{cm}^3$.

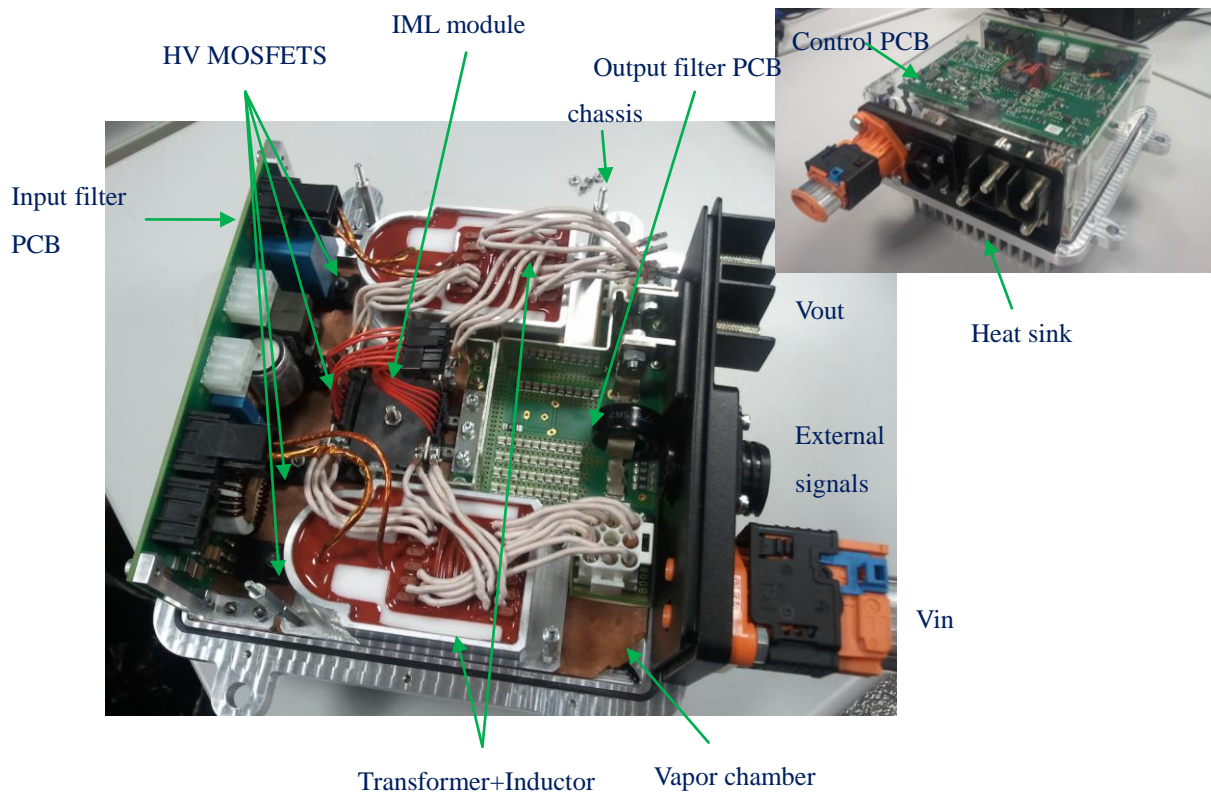


Fig.8. Prototype assembly of LLC converter, water cooled and power density $1\text{W}/\text{cm}^3$

The finally assembled prototype with proposed cooling system is able to operate between -40°C and 60°C with natural convection (maximum component operating temperature $<105^\circ\text{C}$). A forced air-convection of $1.5\text{m}/\text{s}$ is further needed for operating under 70°C ambient temperature, which is the targeted maximum ambient temperature in electric vehicles.

4. Experimental Results

The following figures show the experimental results of the prototype at primary sides and secondary sides:

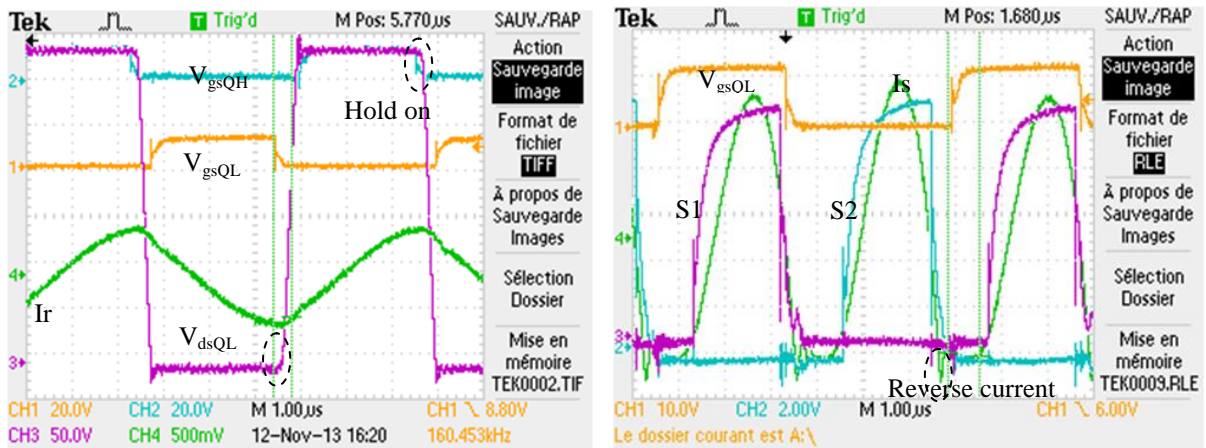


Fig.9. Key operational primary and secondary waveforms for phase B, at $I_o=150A$, $V_{in}=350V$
 ($I_r:10A/div$, $I_s:20A/div$)

The adopted HV super-junction MOSFET (STW88N65M5) performs high nonlinear output capacitor characteristics: C_{oss} is very high at a low V_{ds} . As reported in Fig.9, the drain-source voltage V_{dsQL} is held on at the beginning of ZVS for about 150ns and then the voltage decreases linearly during the dead time, the MOSFETs then can be switched on and off at ZVS. The finally adopted dead time is 400ns. Converter's secondary sides are implemented with synchronous rectifications while the secondary conduction loss is greatly reduced. As reported at the secondary waveforms, the synchronous rectification signal is in phase with the output current and a slight phase lost is detected (synchronous rectification ends 300ns earlier than current falls to zero). A diode conduction loss is expected, but this conduction loss is rather limited considering its conduction time. The reverse recovery current ($\sim 10A$) causes an extra power loss of about 1.5W per FET. Efficiency has been measured and the results are presented as follows:

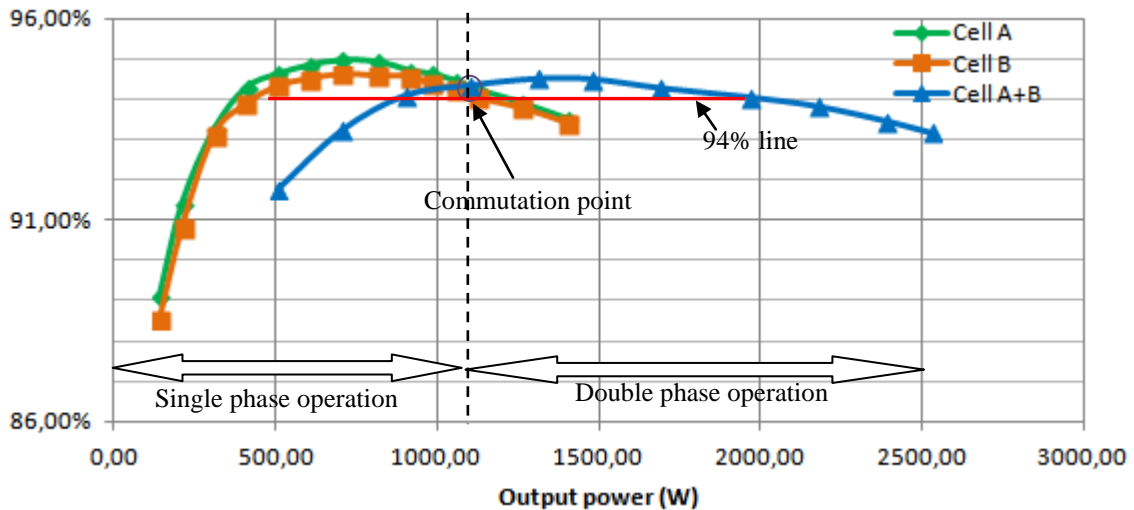


Fig.10. Efficiency measurement results for cells operating alone and cells operating in parallel at
 $V_{in}=330V$, $V_{out}=14V$

The conversion efficiency of a single cell LLC converter is maximal at 700W, with a peak efficiency of 95% for phase A and 94.7% for phase B. Due to the component dispersions, the performance of these two power cells is slightly different. Efficiency begins to decrease when load power exceeds 700W. Setting $P=1.1kW$ as the boundary for single cell operation and double cell operation is a good choice to keep a high efficiency over a high output power

range. When output current exceeds 1.1kW, both the two cells operate and efficiency continues to increase from 1.1kW to 1.5kW.

In all, the designed double phase LLC converter exhibits very good conversion efficiency at a large load variation range: efficiency >94% from 500W to 2kW; Efficiency>93% from 300W to 2.5kW. Even at very low load (140W), the conversion efficiency is quite high: around 89%.

5. Conclusions

The proposed double phase parallel-parallel LLC to handle 180A output current is able to keep a high efficiency at a wide load range. High efficiency at light load is assured by switching off one power cell. In order to avoid the current sharing problems in double phase LLC, double loop control strategy is proposed to equalize the input power of each phase. At the designed prototype, many new implementations for improving the performance of LLC converter are presented. Transformer with E structure integrating magnetizing inductance and partial resonant inductance is a good solution to get a total magnetic volume miniaturization. The air-cooling system with vapor-chamber as heat spreader is effective in rapid and homogenous heat spreading. Fewer semiconductor components, simpler assembly and good current carrying capability can be obtained with the proposed IML power module technology.

In all, the proposed double phase LLC converter is an ideal solution for building HV/LV converters to get a high efficiency and high power density. The final prototype, which can be directly industrialized, adapts perfectly for the applications in DC/DC power conversion for future electric or hybrid vehicles.

6. References

- [1] Bo Yang, "Topology Investigation for Front End DC/DC Power Conversion for Distributed Power System", PhD thesis of Virginia Polytechnic Institute and State University, 2003
- [2] Gang Yang, Patrick Dubus, Daniel Sadarnac, "Design of a high efficiency, wide input range 500kHz 25W LLC resonant converter", Journal of Low Power Electronics, vol. 8, no.4, pp.1-8, August 2012
- [3] Roes, M. G L; Duarte, J.L.; Hendrix, M.A.M., "Disturbance Observer-Based Control of a Dual-Output LLC Converter for Solid-State Lighting Applications," Power Electronics, IEEE Transactions on , vol.26, no.7, pp.2018,2027, July 2011
- [4] H. de Groot, E. Janssen, R. Pagano, K. Schettters, "Design of a 1-MHz LLC Resonant Converter Based on a DSP-Driven SOI Half-Bridge Power MOS Module" IEEE Transactions on Power Electronics, (2007), Vol.22, N° 6, pp.2307-2320.
- [5] M Mao, D Tchobanov, D Li, M Marez, "Analysis and design of a 1MHz LLC resonant converter with coreless transformer driver", PCIM 2007.
- [6] KangHyun Yi; GunWoo Moon, "A novel two phase Interleaved LLC series resonant converter using a phase of the resonant capacitor," Journal of Power Electronics , vol. 8, no.3, pp.275-279, Sept. 27 2008
- [7] C.R. Sullivan, 'Optimal choice for number of strands in a Litz wire transformer winding', IEEE Transactions on Power Electronics, vol. 14, no. 2, 1999
- [8] Correvon, M.; Nagashima, J.; Apter, R., "Power modules with IMS substrates for automotive applications," Vehicular Technology Conference, 2002. VTC Spring 2002. IEEE 55th , vol.4, no., pp.2056,2062 vol.4, 2002
- [9] Dale Mehl, "Vapor chamber heat sinks eliminate power semiconductor hot spots", Power Electronics Technology, Vol. 36, No.8, 2010, pp:16-17